Received: 12 October 2022 | Revised: 18 November 2022 | Accepted: 2 January 2023

DOI: 10.1002/cbin.11989

RESEARCH ARTICLE

Cell Biology International WILEY

Molecular mechanisms on how FABP5 inhibitors promote apoptosis-induction sensitivity of prostate cancer cells

Jiacheng Zhang[1] | Gang He[2] | Xi Jin[3] | Bandar T. Alenezi[1] | Abdulghani A. Naeem[1] | Saud A. Abdulsamad[1] | Youqiang Ke[1,2,3]

[1]Department of Molecular and Clinical Cancer Medicine, Liverpool University, Liverpool, UK

[2]Sichuan Industrial Institute of Antibiotics, Chengdu University, Chengdu, Sichuan, China

[3]Institute of Urology, West China Hospital, Sichuan University, Chengdu, Sichuan, China

Correspondence

Youqiang Ke and Jiacheng Zhang, Department of Molecular and Clinical Cancer Medicine, Liverpool University, the Cancer Research Centre Bldg, 200 London Rd, Liverpool L3 9TA, UK.

Email: yqk@liverpool.ac.uk and aster65@163.com

Abstract

Previous work showed that FABP5 inhibitors suppressed the malignant progression of prostate cancer cells, and this suppression might be achieved partially by promoting apoptosis. But the mechanisms involved were not known. Here, we investigated the effect of inhibitors on apoptosis and studied the relevant mechanisms. WtrFABP5 significantly reduced apoptotic cells in 22Rv1 and PC3 by 18% and 42%, respectively. In contrast, the chemical inhibitor SB-FI-26 produced significant increases in percentages of apoptotic cells in 22Rv1 and PC3 by 18.8% (±4.1) and 4.6% (±1.1), respectively. The bio- inhibitor dmrFABP5 also did so by 23.1% (±2.4) and 15.8% (±3.0), respectively, in these cell lines. Both FABP5 inhibitors significantly reduced the levels of the phosphorylated nuclear fatty acid receptor PPARγ, indicating that these inhibitors promoted apoptosis-induction sensitivity of the cancer cells by suppressing the biological activity of PPARγ. Thus, the phosphorylated PPARγ levels were reduced by FABP5 inhibitors, the levels of the phosphorylated AKT and activated nuclear factor kapper B (NFκB) were coordinately altered by additions of the inhibitors. These changes eventually led to the increased levels of cleaved caspase-9 and cleaved caspase-3; and thus, increase in the percentage of cells undergoing apoptosis. In untreated prostate cancer cells, increased FABP5 suppressed the apoptosis by increasing the biological activity of PPARγ, which, in turn, led to a reduced apoptosis by interfering with the AKT or NFκB signaling pathway. Our results suggested that the FABP5 inhibitors enhanced the apoptosis-induction of prostate cancer cells by reversing the biological effect of FABP5 and its related pathway.

KEYWORDS

AB-FI-26, apoptosis, dmrFABP5, FABP5, PPARγ, prostate cancer

This is an open access article under the terms of the Creative Commons Attribution-NonCommercial License, which permits use, distribution and reproduction in any medium, provided the original work is properly cited and is not used for commercial purposes.

© 2023 The Authors. *Cell Biology International* published by John Wiley & Sons Ltd on behalf of International Federation of Cell Biology.

10958355, 0, Downloaded from https://onlinelibrary.wiley.com/doi/10.1002/cbin.11989 by Test, Wiley Online Library on [18/01/2023]. See the Terms and Conditions (https://onlinelibrary.wiley.com/terms-and-conditions) on Wiley Online Library for rules of use; OA articles are governed by the applicable Creative Commons License

1 | INTRODUCTION

Prostate cancer is the most common male cancer and a serious health threat to men in developed countries (De Angelis et al., 2014; Ferlay et al., 2010). At an early stage, the growth and expansion of prostate cancer depend on the stimulation of the male androgen hormone supplied through peripheral blood. Initially, androgen-deprivation therapy (ADT) can effectively suppress the malignant progression of the cancer cells. But in the majority of prostate cancer cases, the cancer will relapse within about 2 years with a more aggressive androgen-independent form, named castration-resistant prostate cancer (CRPC) (Lee et al., 2008; Miyamoto et al., 2004). The growth and expansion of CRPC no longer rely on androgen anymore. In clinics, ADT is not very effective against CRPC and currently CRPC is not a curable disease. Therefore, identification and validation of novel therapeutic targets is an imperative task for development of an effective treatment of CRPC.

One of the genes involved in promoting malignant progression of prostate cancer cells is *fatty acid-binding protein 5* (*FABP5*) (McKillop et al., 2019; Morgan et al., 2008). FABP5 is a member of the fatty acid-binding protein (FABP) family and is a 15 kDa cytosolic protein that binds, with a high affinity, to long and middle chain fatty acids (Cucchi et al., 2019; Liu & Godbout, 2020; Madsen et al., 1992). Previous studies have suggested that the increased level of FABP5 in prostate cancer cells can transport a large amount of intracellular and extracellular fatty acids into the cytoplasm to be used as alternative energy sources during ADT. The excessive amount of fatty acids can then act as signaling molecules to stimulate the nuclear fatty acid receptor PPARγ (Liu & Choi, Jain, et al., 2020). The activated PPARγ (phosphorylated PPARγ or p-PPARγ) can trigger a chain of molecular events, which include an upregulation of the regulatory cancer-promoting genes, such as that for vascular endothelial growth factor (VEGF) (Adamson et al., 2003; Gujrati et al., 2022), and a downregulation of possible cancer-suppressing genes, eventually leading to an enhanced malignant progression of the cancer cells (Bao et al., 2013; Biswas et al., 2022). Our previous study showed that the FABP5-PPARγ-signaling transduction axis gradually replaced the androgen receptor (AR)-related signal pathway and eventually became dominant in CRPC cells. Thus suppressing the FABP5-PPARγ-signal pathway, rather than the AR-related pathway alone, may be a more relevant strategy for the treatment of CRPC (Forootan et al., 2014, 2016; Naeem et al., 2019).

Our previous studies showed that apoptosis was reduced as the overexpression of FABP5 in prostate cancer cells (Li et al., 1998). It was suggested that the suppression in apoptosis, like the increase in VEGF, may be a consequence of activated- or p-PPARγ resulting from the stimulation of fatty acids transported by the elevated FABP5 (Bao et al., 2013, Forootan et al., 2016). Moreover, activation of the AKT pathway may produce an antiapoptotic effect by reducing PTEN-mediated apoptosis (Li et al., 1998). It has been reported that AKT can prevent cancer cells from cell death by activating several apoptosis-related factors (Vivanco & Sawyers, 2002). For example, the phosphorylation of AKT inhibits caspase-9, a prodeath protease in human cells (Cardone et al., 1998). Although it was shown that the AKT-signal transduction pathway was functioning in prostate cancer (Li et al., 1998), it is not clear whether the FABP5-PPARγ-signal pathway in prostate cancer is connected to that of the AKT-pathway.

Apart from the initial discovery that FABP5 is overexpressed in prostate carcinomas and plays a crucial role in promoting malignant progression (Jing et al., 2000; Jing et al., 2001), the involvement of FABP5 in many other types of solid tumors has also been reported. Thus, FABP5 is likely to be a general promoting factor for carcinogenesis of most solid carcinomas (Al-Jameel et al., 2017; Fujii et al., 2005; Furuhashi et al., 2007; Levi et al., 2015; Sinha et al., 1999; Vorum et al., 1998). The increased level of FBAP5 may cause an increase in some cancer-promoting genes, such as VEGF, through activation of PPARγ by the stimulation of fatty acids transported by FABP5 (Al-Jameel et al., 2019). Although a previous study has suggested the possibility that the increased level of FABP5 in prostate cancer cells promotes malignant progression by suppressing apoptosis (Bao et al., 2013), confirmation on this point is needed and the molecular mechanism of how the increased FABP5 can affect apoptosis is not known.

In a previous study, a chemically-synthesized FABP5 inhibitor SB-FI-26 was used to treat CRPC in a nude mouse model and this compound produced a significant reduction in the primary tumor mass by more than ninefold and significantly inhibited metastasis by 50% (Al-Jameel et al., 2017, Carbonetti et al., 2020). More recently, we have used dmrFABP5, a bio-inhibitor for FABP5, to treat CRPC in an experimental nude mouse model. DmrFABP5 was obtained by changing (through creating mutations to the gene codons) 2 of the 3 key amino acids in the fatty acid-binding motif of the wide type FABP5. These changes almost completely deprived of the fatty acid-binding ability of FABP5 and thus, dmrFABP5 can competitively reduce the fatty acid transportation by FABP5 and hence suppress tumorigenicity of the cancer cells by reducing cellular fatty acid uptake. Experimental treatment with dmrFABP5 produced more than a 13-fold reduction on average primary tumor mass and 100% inhibition of metastasis (Al-Jameel et al., 2019). In this study, we investigated whether these inhibitors suppress malignant progression of the CRPC cells, either in whole or in part, by promotion of apoptosis in the cancer cells and the details of the relevant signaling pathways involved.

2 | MATERIALS AND METHODS

2.1 | Cell lines and culture conditions

The following three human prostate cell lines were used in this study: the benign prostate epithelial cell line PNT-2 (Berthon et al., 1995; Cussenot et al., 1991; Cussenot et al., 1994), the moderately malignant AR^+ CRPC cell line 22Rv1 (Sramkoski et al., 1999) and the highly malignant AR^- CRPC cell line PC3 (Kaighn et al., 1978). Cells were grown and maintained in a monolayer culture in RPMI 1640 medium ((Life Technologies), supplemented with 10% (vol/vol)

10958355, 0, Downloaded from https://onlinelibrary.wiley.com/doi/10.1002/cbin.11989 by Test, Wiley Online Library on [18/01/2023]. See the Terms and Conditions (https://onlinelibrary.wiley.com/terms-and-conditions) on Wiley Online Library for rules of use; OA articles are governed by the applicable Creative Commons License

fetal calf serum (Biosera), L-glutamine (20 mM) (Invitrogen), penicillin (100 U/ml) and streptomycin (100 µg/ml) (Biosera).

2.2 | Expression of FABPs in *Escherichia coli* cells

The procedures used for production of wtrFABP5 and dmrFABP5 were the same as those described previously (Al-Jameel et al., 2019). A single colony was picked from a selective antibiotic LB agar plate, inoculated into 10 ml LB medium containing 50 µg/ml ampicillin in a 50 ml flask and incubated at 37°C overnight with a shaking (230 rpm) incubator. The overnight bacterial culture (10 ml) was transferred to a flask containing prewarmed medium (250 ml) with ampicillin and grown at 37°C with vigorous shaking until the OD_{600} reached 0.6. Expression of the recombinant proteins was induced by adding IPTG (Isopropylthiogalactoside) (Sigma) to a final concentration of 1 mM. The flask was incubated for an additional 4 h, the time at which the maximum amount of protein was synthesized. Cells were harvested by centrifugation at 4000*g* for 20 min and pellets were stored at −20°C until further use.

2.3 | Protein purification

Purification of Hexa-His-tagged proteins under native condition was conducted with a Ni-NTA Fast Start kit (Qiagen). Cell pellets were suspended in 10 ml Lysis Buffer (pH 8.0), incubated at room temperature for 60 min and then centrifuged at 14,000*g* for 30 min at 4°C to pellet the cellular debris. The supernatant containing the recombinant protein was separated from the debris, collected and loaded onto a Ni-NTA column containing a Hexa-His antibody. After 2 washes with 4 ml of Washing Buffer (pH 8.0), the recombinant protein bound to Hexa × His-tagged antibody was eluted with an elution buffer (pH 8.0). Each of the 2 eluted fractions was collected and the protein in the eluted fractions was subjected to SDS-PAGE and Western blot analysis to confirm their authenticity, as described previously (Al-Jameel et al., 2019) (Data not shown).

2.4 | Measurement of apoptotic cells

Cells growing in culture medium were initially treated with camptothecin to induce apoptosis, and then treated with SB-FI-26, wtrFABP5 or dmrFABP5 to study their effect on apoptosis-induction sensitivity. Those cells undergoing apoptosis were stained by an annexin V-FITC Apoptosis Detection Kit, following the manufacturer's instructions (Sigma-Aldrich) (Annexin V can conjugate to phosphatidyl serine, which translocates it from the inner plasma membrane to the cell surface at an early stage of apoptosis). The percentage of cells undergoing apoptosis was identified and calculated by flow cytometry using a FACSCanto II Flow Cytometer (BD).

2.5 | Western blot

Levels of proteins in control cells and cells treated with wtrFABP5 or dmrFABP5 were detected by Western blot using an ECL detection system (Millipore) (Forootan et al., 2006; Ke et al., 1997). Proteins were separated by SDS-PAGE in a 12.5% (w/v) acrylamide gel, and transferred onto a nitrocellulose membrane (Hybond ECL, Amersham Pharmacia). The primary antibody against p-PPARγ (Ser 112) (Thermo Fisher) was diluted at 1:200 and incubated with the blot overnight. After incubating with horseradish peroxidase-conjugated anti-rabbit IgG (Santa-cruz) diluted at 1: 10,000, protein bands were detected and measured by exposing the membrane in an imaging analysis machine (ChemiDoc MP Imaging System; Bio-Rad). The primary antibodies against PPARγ, AKT, p-AKT (Ser^{473}), BAX, Bcl-2, the cleaved-Capase-9 and the cleaved-Caspase-3 (Cell Signaling) were diluted at 1:200−500 and incubated with the blots for 1 h. After incubating with horseradish peroxidase-conjugated anti-rabbit (AKT, p-AKT and cleaved-caspase-3)—or anti-mouse (PPARγ, BAX, Bcl-2, cleaved-caspase-9)—IgG diluted at 1:10,000, respectively, protein bands were detected and measured in the same way as p-PPARγ. The antibody against β-actin was used to quantify the actin bands on each blot to correct for possible loading discrepancies. Both the unphosphorylated and phosphorylated forms of AKT and PPARγ were quantitated with relating to actin in the same way.

2.6 | NFκB transcription factor assay

The DNA binding activity of nuclear factor kapper B (NFκB) in the cell nucleus was detected by an NFκB p65 transcription factor assay kit (Abcam). Nuclear extracts of control cells (treated with PBS) and cells treated with wtrFABP5 or dmrFABP5 were collected using a nuclear extraction kit (Abcam), following the manufacturer's instructions. Nonspecific binding wells, positive control wells, specific competitor double-stranded DNA (dsDNA) wells and test wells were set up in duplicates in a transcription factor NFκB 96-well strip plate. In test groups, each well was first coated with a consensus double-stranded DNA (dsDNA), the transcription factor was bound specifically to the dsDNA; the plate was then washed, treated with NFκB primary antibody (1: 100). The wells were then washed and incubated with a goat anti-rabbit HRP antibody (1:100). After the transcription factor-developing solution was added to each well for 30 min in the dark, the stop solution was added and absorbance at 450 nm measured within 5 min.

2.7 | Statistical analysis

Student's *t*-test was carried out using GraphPad Prism software to compare the differences of the means between control and experimental groups and the data is presented as mean ± SE. The *P*-value less than 0.05 was regarded as statistical significance $^{*}p < .01$; $^{**}p < .001$(***).

10958355, 0, Downloaded from https://onlinelibrary.wiley.com/doi/10.1002/cbin.11989 by Test, Wiley Online Library on [18/01/2023]. See the Terms and Conditions (https://onlinelibrary.wiley.com/terms-and-conditions) on Wiley Online Library for rules of use; OA articles are governed by the applicable Creative Commons License

3 | RESULTS

3.1 | Wild type recombinant (wtr) FABP5 suppresses apoptosis-induction sensitivity of the CRPC cells

The AR$^+$ CRPC cell line 22Rv1 and the AR$^-$ CRPC cell line PC3 were treated with wtrFABP5 to study its effect on apoptosis-induction sensitivity (Figure 1). As shown in Figure 1 (the inserts a–d), wtrFABP5 treatment reduced apoptosis induced by camptothecin in both cell lines. Quantitative analysis of flow cytometry results before the wtrFABP5 treatment showed that the apoptotic rate induced by camptothecin in the moderately malignant 22Rv1 cells was significantly higher than that of the highly malignant PC3 cells by 2.54% (Student's *t*-test, $p < .01$) (Figure 1). When treated with wtrFABP5, all doses produced reductions in apoptosis-induction and the highest reduction was achieved in both cell lines with 0.5 μM wtrFABP5. Further increase in dose produced little further noticeable reduction in apoptosis-induction (Figure 1). When treated with this optimal dose of wtrFABP5 in 22Rv1 cells, 15.9% of cells underwent apoptosis, a significant reduction from 19.4% in the control treated with camptothecin only (Student's *t*-test, $p < .05$), the wtrFABP5 treatment reduced the apoptotic fraction of the cells by 3.5% in 22Rv1 cultures. Thus, in wtrFABP5-treated 22Rv1 cells, the number of cells undergoing apoptosis was reduced by 18%. In PC3 cells, the optimal dose of wtrFABP5 reduced by 7.1% of the fraction of cells undergoing apoptosis (Student's *t*-test, $p < .05$) when compared to that of the control (16.9%). Thus, in wtrFABP5-treated PC3, the number of apoptotic cells induced by comptothecin was reduced by 42%.

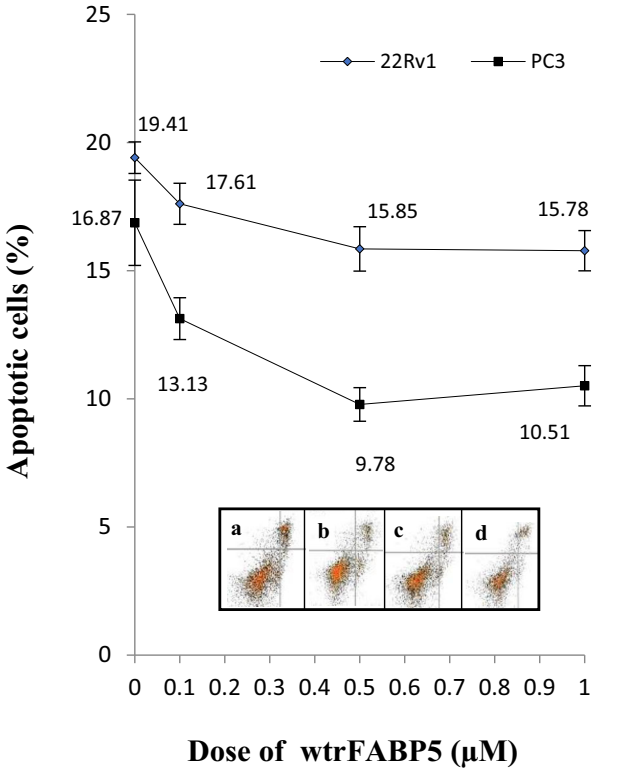

FIGURE 1 The effect of wtrFABP5 on induction of apoptosis of prostate cancer cells. The surface of cells undergoing apoptosis was stained with antibodies to annexin-V (bound to phosphatidylserine, which translocates from the inner plasma membrane to the cell surface at an early stage of apoptosis) and was measured by flow cytometry of intact cells. The AR$^+$ CRPC cell line 22RV1 and the AR$^-$ CRPC cell line PC3 were cultured to 90% confluence and harvested. Equal numbers (1×10^5) of cells were then sub-cultured in triplicates with camptothecin (5 ng/ml). Each different dose of wtrFABP5 was added to each of the triplicate cultures and the cells were allowed to grow for a further 48 h. The percentages of the apoptotic cells in 22RV1 and PC3 cell lines were measured after the treatment with 4 different doses of wtrFABP5 respectively. The results were obtained from 3 (mean ± SD) separate experiments. Inserts: Representative dot graphs of percentages of apoptotic cells from the control and the cells treated with the optimal dose (0.5 μM) of wtrFABP5. For each dot graph, dots in the first quadrant (upper right) represent the late stage apoptotic cells. Dots in the second quadrant (upper left) represent dead cells and cell debris. Dots in the third quadrant (lower left) represent normal living cells, which do not undergo apoptosis. Dots in the fourth quadrant (lower right) represent cells undergoing apoptosis. (a), dot graph record of control 22RV1 cells (treated with PBS). (b), dot graph record of control PC3 cells (treated with PBS). (c), dot graph record of 22RV1 cells treated with 0.5 μM wtrFABP5. (d), dot graph record of control PC3 cells treated with 0.5 μM wtrFABP5.

3.2 | FABP5 inhibitors promote apoptosis-induction of the CRPC cells

The effect of FABP5 inhibitors SB-FI-26 and dmrFABP5 on apoptosis-induction sensitivities of 22Rv1 and PC3 cells was studied (Figure 2). As shown in the inserts a–d in A and the inserts a–d in B respectively, both inhibitors promoted apoptosis-induction sensitivity of both cell lines used. Quantitative analysis showed that all doses of SB-FI-26 produced increases in apoptosis-induction and the increase was positively correlated to the increase in dose (Figure 2A). When 22Rv1 cells were treated with the maximum dose (150 μM) of SB-FI-26, 47.9% of cells underwent apoptosis, a significant increase of 26.4% over that (21.5%) in the control treated by camptothecin alone (Student's *t*-test, $p < .001$). Thus, SB-FI-26 produced 123% more apoptotic cells in the 22Rv1 culture (A). In PC3 cells, the maximum dose (150 μM) of SB-FI-26 significantly increased by 14.3% in the percentage of cells undergoing apoptosis (Student's *t*-test, $p < .05$) when compared to that of the control (16.9%). Thus, there were 78% more cells undergoing apoptosis in SB-FI-26-treated PC3 cells in comparison to the control treated by comptothecin alone (A). Quantitative analysis of flow cytometry results showed that when treated with different doses of dmrFABP5, all doses increased apoptosis-induction sensitivity and the highest increase was achieved in both cell lines with 0.5 μM dmrFABP5. Further increase in dmrFABP5 produced no further significant increase in apoptosis. When treated with this optimal dose of dmrFABP5 in 22Rv1 cells, 38.8% of cells underwent apoptosis, a significant increase by 19.4% over that (19.4%) in the control (Student's *t*-test, $p < .001$). Thus,

10958355, 0, Downloaded from https://onlinelibrary.wiley.com/doi/10.1002/cbin.11989 by Test, Wiley Online Library on [18/01/2023]. See the Terms and Conditions (https://onlinelibrary.wiley.com/terms-and-conditions) on Wiley Online Library for rules of use; OA articles are governed by the applicable Creative Commons License

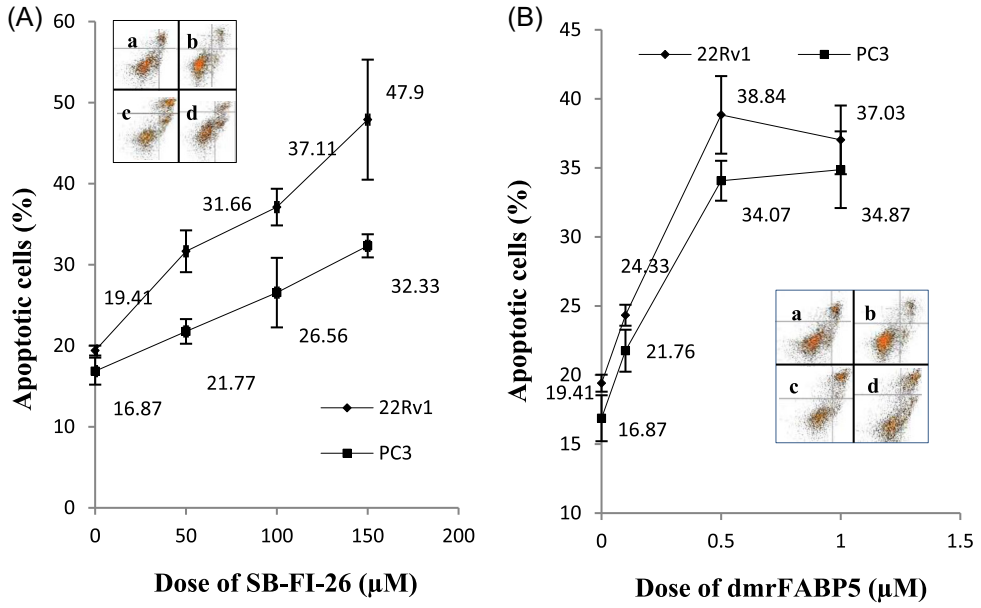

FIGURE 2 The effect of SB-FI-26 and dmrFABP5 on induction of apoptosis of prostate cancer cells. The surface of cells undergoing apoptosis was stained with antibodies to annexin-V and was measured by flow cytometry of intact cells. Cell lines 22Rv1 and PC3 were cultured to 90% confluence and harvested. Equal numbers (1×10^5) of cells were then sub-cultured in triplicate with camptothecin (5 ng/ml). Each different dose of SB-FI-26 and dmrFABP5 was added to each of the triplicate cultures and the cells were allowed to grow for 48 h. (A) Percentages of the apoptotic cells in 22RV1 and PC3 cell lines treated with 4 different doses of SB-FI-26. Inserts: Representative dot graph records of percentages of apoptotic cells from the control and the cells treated with SB-FI-26 (100 μM). (a), dot graph record of control 22RV1 cells (treated with PBS). (b), dot graph record of control PC3 cells (treated with PBS). (c), dot graph records of 22RV1 cells treated with 100 μM SB-FI-26. (d), dot graph record of control PC3 cells treated with 100 μM SB-FI-26. (B) Percentages of apoptotic cells in 22RV1 and PC3 cell lines treated with four different doses of dmrFABP5. The results were obtained from 3 (mean ± SD) separate experiments. The levels in the negative control wells were set at 1 and the remaining were calculated in relation to the negative control. Inserts: Representative dot graph records of percentages of apoptotic cells from the control and the cells treated with the optimal dmrFABP5 dose (0.5 μM). (a), dot graph record of control 22RV1 cells (treated with PBS). (b), dot graph record of control PC3 cells (treated with PBS). (c), dot graph record of 22RV1 cells treated with 0.5 μM dmrFABP5. (d), dot graph record of control PC3 cells treated with 0.5 μM dmrFABP5.

dmrFABP5 treatment produced 100% more apoptotic cells in the 22Rv1 cultures. In PC3 cells, the optimal dose of dmrFABP5 produced 34.1% of cells undergoing apoptosis; an increase in the percentage of cells undergoing apoptosis by 17.2% (Student's *t*-test, $p < .001$) when compared to that of the control treated with comptothecin alone (16.9%) (B). Thus dmrFABP5 produced 102% more cells undergoing apoptosis.

3.3 | Levels of PPARγ and AKT in benign and malignant prostate epithelial cells

Levels of PPARγ, AKT, and their phosphorylated forms (presumably bioactive) p-PPARγ and p-AKT were measured by Western blot and the levels relative to actin were shown in Figure 3a,c,e,g. Levels of both PPARγ and AKT in the benign PNT2 cells were much higher than those in the malignant 22Rv1 and PC3 cells (Figure 3b,f). However, the proportions of their phosphorylated forms were greatly increased in the malignant cells compared to those in benign PNT2 cells. When the level of p-PPARγ was set at 1 in PNT2 cells, its relative level was greatly increased by 18.74 ± 2.46 and 16.47 ± 1.45 ford in 22Rv1 and PC3 cells, respectively (D). When the level of p-AKT was set at 1 in PNT2 cells, its relative level was increased by 1.27 ± 0.09 and 2.57 ± 0.3 in 22Rv1 and PC3 cells, respectively (H).

3.4 | Levels of apoptosis-pathway-related factors in benign and malignant prostate epithelial cells

Levels of several factors related to apoptosis signal transduction in benign and malignant prostate epithelial cells were measured by Western blot (Figure 4). Bands for BAX, Bcl-2 cleaved-caspase-9 and cleaved-caspase-3 were detected in all three cell lines (a,c,e,g). Quantitative analysis showed that the levels of BAX in PNT2, 22Rv1, and PC3 were very different. When the level in the benign PNT2 cells was set at 1, its relative levels in 22Rv1 and PC3 cells were 0.49 ± 0.08 and 0.31 ± 0.02, respectively (b); significant reductions by 51% and 61%, respectively (Student's *t*-test, $p < .005$). The levels of Bcl-2 in these 3 cell lines were very similar (d). For cleaved-caspase-9, the expression pattern in these 3 cell lines was different from that of Bcl-2. When the level of cleaved-caspase-9 in PNT2 was set at 1, its relative levels in 22Rv1 and PC3 were 0.97 ± 0.06 and 0.69 ± 0.03, respectively (f). While the levels between PNT2 and 22Rv1 cells were very similar, the cleaved-caspase-9 level in the highly malignant PC3

10958355, 0, Downloaded from https://onlinelibrary.wiley.com/doi/10.1002/cbin.11989 by Test, Wiley Online Library on [18/01/2023]. See the Terms and Conditions (https://onlinelibrary.wiley.com/terms-and-conditions) on Wiley Online Library for rules of use; OA articles are governed by the applicable Creative Commons License

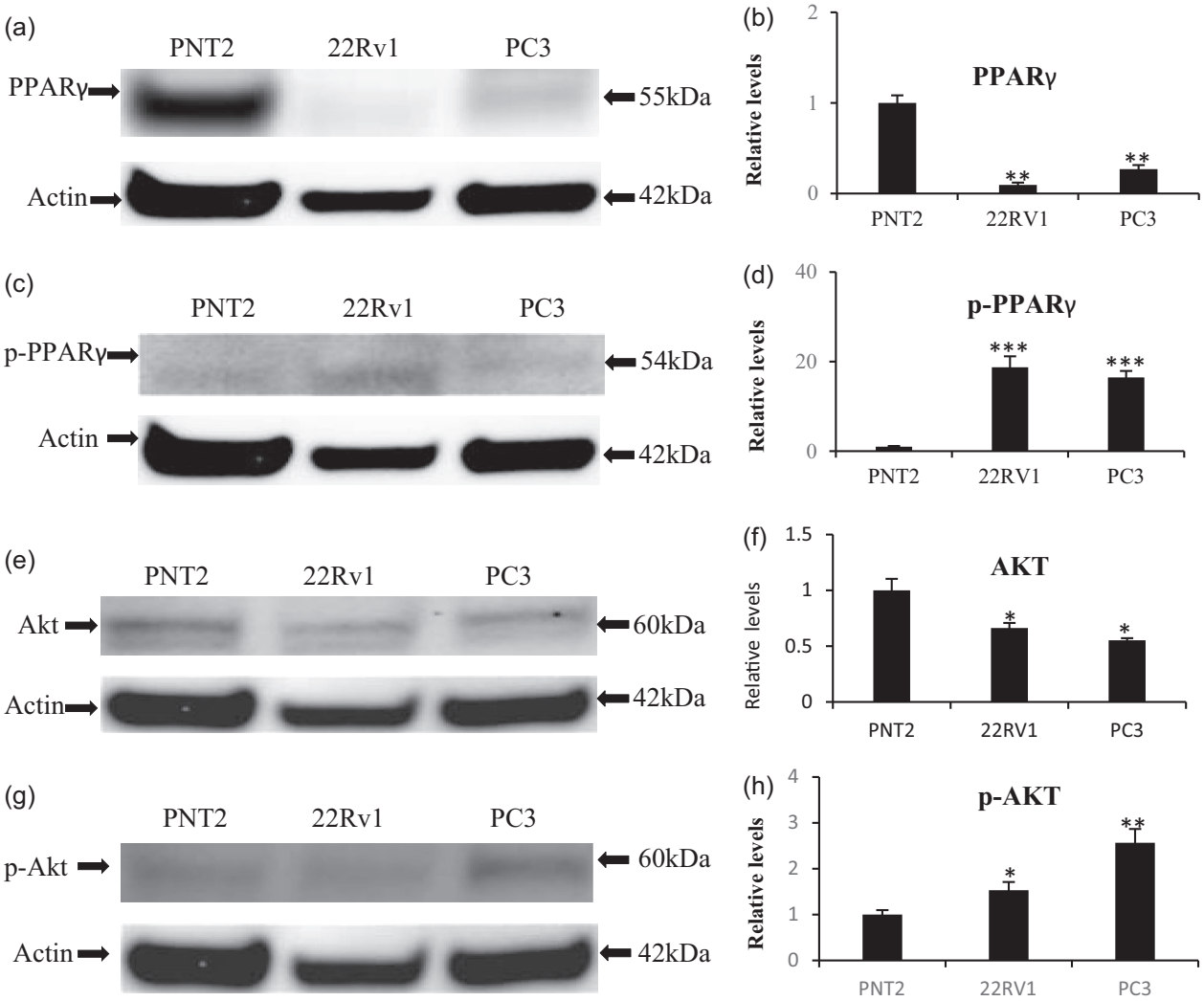

FIGURE 3 The levels of PPARγ, p-PPARγ, AKT, and p-AKT in benign and malignant prostate epithelial cells by Western blot. The benign cell line PNT2, the prostate cancer cell lines 22RV1 and PC3 were cultured to 90% confluence, harvested and disrupted with cell lysis buffer. The cell extracts were first subjected to SDS-Page and then Western blot analysis. An antibody against nonmuscle β-actin was incubated with each blot to correct possible loading discrepancies and for standardization purposes. (a, c, e, and g) Western blot analyses of PPARγ, p- PPARγ, AKT, p-AKT expression in the benign PNT2 cells and in the malignant 22RV1 and PC3 cells. (b, d, f, and h) Quantitative assessments of the relative levels of PPARγ, p-PPARγ, AKT, p-AKT by densitometric scanning of the intensities of the bands on each blot relative to those of actin. The results were obtained from 3 (mean ± SD) separate experiments. The level of each of the 4 proteins in the benign PNT2 cells were set at 1; the levels of the other cell lines on the same blot were calculated by relating to that of PNT2.

cells was significantly (Student's *t*-test, $p < .01$) reduced by 31% when compared to that in the benign PNT2 cells. For cleaved-caspase-3, when the level in PNT2 was set at 1, its relative levels in 22Rv1 and PC3 were 0.54 ± 0.09 and 0.42 ± 0.03, respectively (f), a significant reduction by 46% and 58%, respectively (Student's *t*-test $p < .01$; $p < .05$).

3.5 | The effect of dmrFABP5 on levels of PPARγ, AKT, and other apoptosis-related factors in PC3 cells

The effect of dmrFABP5 on levels of PPARγ and AKT in PC3 cells was measured by Western blot (Figure 5). As shown in A-a and A-e, wtrFABP5 and dmrFABP5 separately produced no noticeable changes in the sizes of the bands and the quantitative assessments showed that neither wtrFABP5 nor dmrFABP5 treatment produced significant changes in the levels of both PPARγ (Student's *t*-test, $p > .05$) and AKT ($p > .1$) (B-a and B-e). Treatment with wtrFABP5 increased the expression of p-AKT and p-PPARγ in relative to actin (A-b and A-c). Quantitative analysis showed that wtrFABP5 produced a significant increase (Student's *t*-test, $p < .001$) in the level of p-AKT (B-b) by 69%, and a significant increase (Student's *t*-test, $p < .001$) in p-PPARγ (B-c) level by 39%. When PC3 cells were treated with dmrFABP5 (A-b and A-c), significant reductions (Student's *t*-test, $p < .05$, $p < .001$) were produced in levels of p-AKT by 21% and in p-PPARγ by 48% (B-b and B-c), respectively. When the PC3 cells were treated with wtrFABP5 and dmrFABP5, the intensities

10958355, 0, Downloaded from https://onlinelibrary.wiley.com/doi/10.1002/cbin.11989 by Test, Wiley Online Library on [18/01/2023]. See the Terms and Conditions (https://onlinelibrary.wiley.com/terms-and-conditions) on Wiley Online Library for rules of use; OA articles are governed by the applicable Creative Commons License

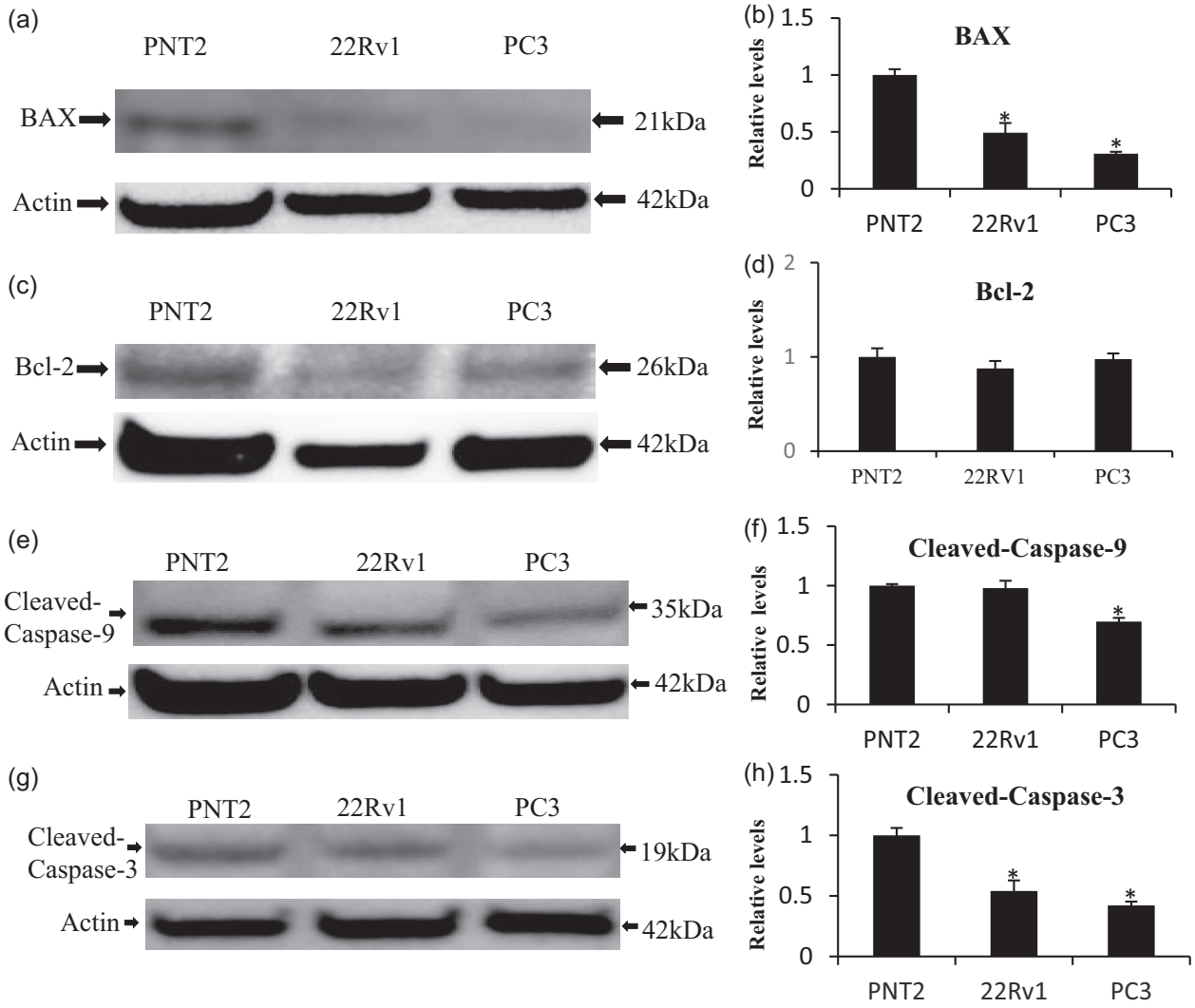

FIGURE 4 The levels of BAX, Bcl-2, cleaved-caspase-9 and cleaved-caspase-3 in benign and malignant prostate epithelial cells determined by Western blot. An antibody against non-muscle β-actin was incubated with each blot to correct loading discrepancies and for standardization purposes. (a, c, e, and g) Western blots of BAX, Bcl-2, cleaved-caspase-9, and cleaved-caspase-3 in benign PNT2 cells and in malignant 22RV1 and PC3 cells. (b, d, f, and h) Quantitative assessments of the relative levels of BAX, Bcl-2, cleaved-caspase-9 and cleaved-caspase-3 by densitometric scanning of the intensities of the bands on each blot relative to those of actin (b, d, f, and h). The results were obtained from 3 (mean ± SD) separate experiments. For each of the 4 proteins, the levels in the benign PNT2 cells were set at 1; the levels in the other cell lines on the same blot were calculated by relating to those in PNT2.

of the bands representing cleaved-caspase-9 and cleaved-caspase-3 respectively changed (A-d and A-f). When the level of cleaved-caspase-9 in the control (treated with PBS) was set at 1 (B-d); its relative level in cells treated with wtrFABP5 was reduced to 0.39 ± 0.05; a significant (Student's *t*-test, $p < .001$) reduction by 61%. In contrast, the relative level in cells treated with dmrFABP5 was significantly (Student's *t*-test, $p < .001$) increased by 31% to 1.31 ± 0.11. Treatment with both wtrFABP5 and dmrFABP5 produced a reduction in levels of cleaved-caspase-9 by 31%, which was a significant reversal of the effect of wtrFABP5 alone. Further quantitative analysis showed that the dmrFABP5-treated PC3 cells produced a remarkable change in cleaved-caspase-3 level (B-f). When the level of the cleaved-caspase-3 was set at 1; its relative level in cells treated with wtrFABP5 was 0.36 ± 0.06, a significant reduction by 64% (Student's *t*-test, $p < .001$). The relative level of the cleaved-caspase-3 in PC3 cells treated with dmrFABP5 was increased to 1.23 ± 0.14, a significant increase of 23% (Student's *t*-test, $p < .001$). Treatment with both wtrFABP5 and dmrFABP5 produced no significant difference compared to untreated control PC3 cells.

3.6 | The effect of wtrFABP5 and dmrFABP5 on levels of BAX and Bcl-2 and on NF-κB activity in PC3 cells

The effect of wtrFABP5 and dmrFABP5 on levels of BAX and Bcl-2 was detected by Western blot and quantitative assessments were

10958355, 0, Downloaded from https://onlinelibrary.wiley.com/doi/10.1002/cbin.11989 by Test, Wiley Online Library on [18/01/2023]. See the Terms and Conditions (https://onlinelibrary.wiley.com/terms-and-conditions) on Wiley Online Library for rules of use; OA articles are governed by the applicable Creative Commons License

shown in Figures 6 (a,b,c, and d). When BAX level in the control cells was set at 1; its relative level in cells treated with wtrFABP5 was reduced significantly (Student's *t*-test, $p < .001$) by 34% to 0.66 ± 0.17 (c), whereas the relative level of BAX in the cells treated with dmrFABP5 was significantly (Student's *t*-test, $p < .001$) increased by 45% to 1.45 ± 0.22 (c). Treatment with both wtrFABP5 and dmrFABP5 produced no significant difference compared to the untreated control cells. When the level of Bcl-2 in the control cells

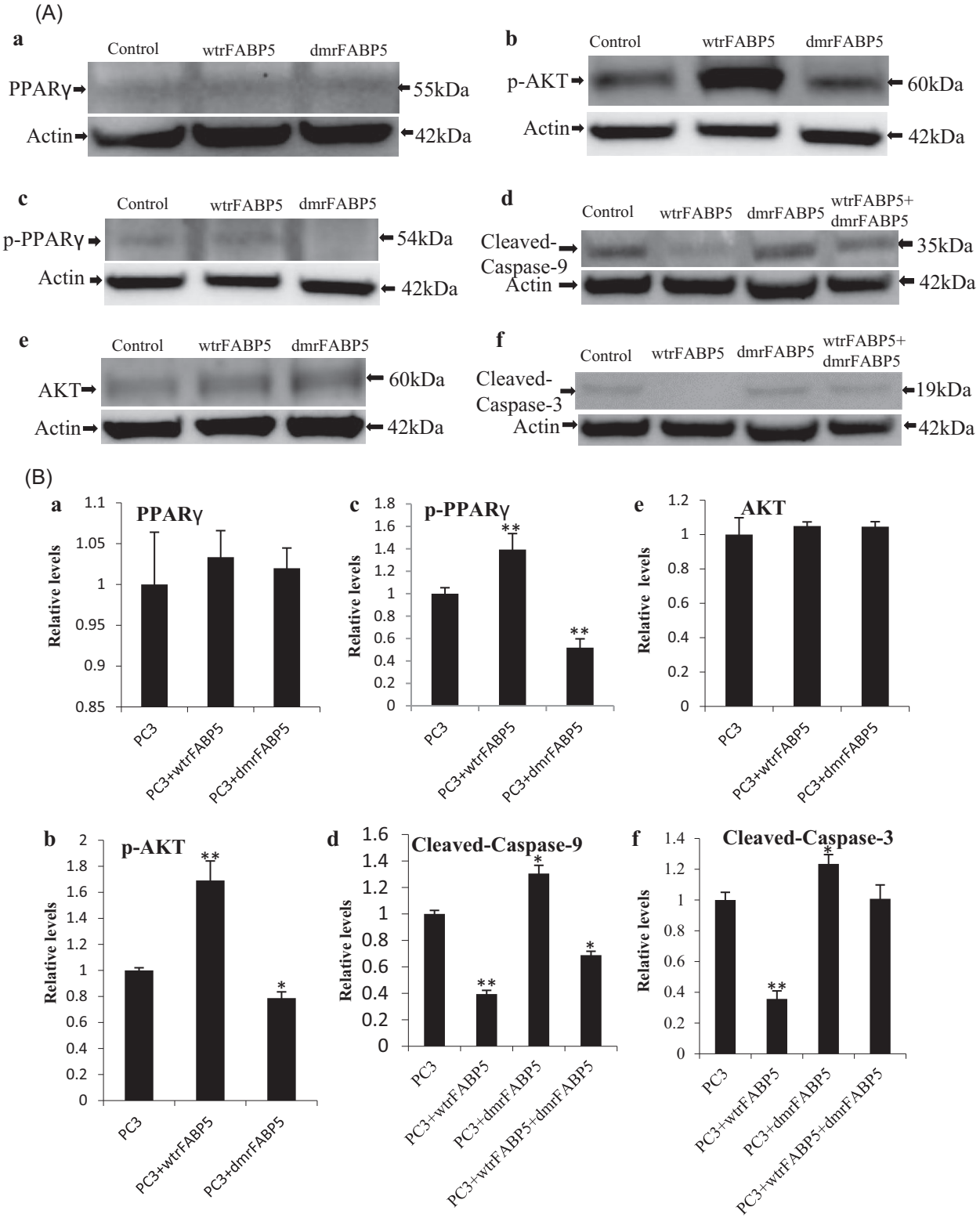

FIGURE 5 (See caption on next page)

10958355, 0, Downloaded from https://onlinelibrary.wiley.com/doi/10.1002/cbin.11989 by Test, Wiley Online Library on [18/01/2023]. See the Terms and Conditions (https://onlinelibrary.wiley.com/terms-and-conditions) on Wiley Online Library for rules of use; OA articles are governed by the applicable Creative Commons License

was set at 1; its relative level in cells treated wtrFABP5 was significantly (Student *t*-test, $p < .0001$) increased by 4.16 ± 0.32-fold, whereas its level in cells treated with dmrFABP5 was significantly (Student's *t*-test, $p < .005$) reduced by 44% to 0.56 ± 0.19-fold. Treatment with both wtrFABP5 and dmrFABP5 produced no significant difference compared with the untreated control cells. To assess the ratio of BAX/Bcl-2 (Figure 6e), the ratio in control cells was set at 1. While the BAX/Bcl-2 ratio in cells treated with wtrFABP5 was significantly (Student's *t*-test, $p < .0001$) reduced by 89% to 0.11 ± 0.02, this ratio in cells treated with dmrFABP5 was significantly (Student's *t*-test, $p < .0001$) increased by 60% to 1.6 ± 0.28. Treatment with both wtrFABP5 and dmrFABP5 produced no significant change in their ratio compare with the untreated control cells. The effect of wtrFABP5 and dmrFABP5 on NF-κB transcription factor activity in PC3 cells was assessed with a transcription factor-binding assay. As shown in f, when the level of NF-κB transcription factor activity in the benign PNT2 cells was set at 1; the level in the PC3 cells was significantly (Student's *t*-test, $p < .05$) increased to 1.09 ± 0.02. The treatment of the PC3 cells with wtrFABP5 significantly (Student's *t*-test, $p < .0001$) increased the NF-κB transcription factor activity by 24.77% to 1.36 ± 0.01. The treatment with dmrFABP5 significantly (Student's *t*-test, $p < .0005$) reduced NF-κB transcription factor activity in PC3 cells by 27.61% to 0.80 ± 0.05.

4 | DISCUSSION

To study the relationship between FABP5 and cell apoptosis, the moderately malignant, AR^+ 22Rv1 CRPC cells and the highly malignant, AR^-PC3 CRPC cells were first treated with the apoptosis-inducer camptothecin and then with wtrFABP5 or with two FABP5 inhibitors separately: either SB-FI-26 or dmrFABP5. DmrFABP5 is a recombinant protein obtained by mutating 2 of the 3 codons (in the FABP5 cDNA) for the 3 key amino acids (Arg^{109}, Arg^{129}, Tyr^{131}) of the fatty acid-binding motif. Thus, dmrFABP5 has a very similar structure to that of wtrFABP5, but is incapable of binding to fatty acids (Al-Jameel et al., 2019). Our previous studies showed that either inhibitor significantly suppressed the tumorigenicity and metastasis of experimental prostate cancer (Al-Jameel et al., 2017, 2019). In this work, treatment with wtrFABP5 suppressed apoptosis significantly in both 22Rv1 and PC3 cells. The SB-FI-26 treatment caused 123% and 78% more cells to undergo apoptosis in 22Rv1 and PC3 cells, respectively. Treatments with dmrFABP5 triggered 100% and 102% more cells to undergo apoptosis in 22Rv1 and PC3 cells, respectively. These results showed that the increased level of FABP5 suppressed apoptosis-induction sensitivity of the prostate cancer cells. In contrast, the opposite effect was observed by treatment with either inhibitor SB-FI-26 or dmrFABP5, suggesting that both FABP5 inhibitors suppressed prostate cancer by promoting the ability of cancer cells to undergo apoptosis.

SB-FI-26, as an inhibitor of FABP5, exhibited an ability to suppress both tumorigenicity and metastasis of prostate cancer (Al-Jameel et al., 2017). It can competitively bind to FABP5 to prevent intracellular and extracellular fatty acids from being transported into the cytoplasm and hence to reduce the cellular fatty acid uptake (Al-Jameel et al., 2017). When treated with SB-FI-26, FABP5 can no longer transport and deliver fatty acids to the nuclear receptor PPARγ and thus it prevents the fatty acids from stimulating and activating PPARγ. Therefore, SB-FI-26 suppresses malignant progression of prostate cancer cells by reducing the level of p-PPARγ. Since SB-FI-26 has been identified as a weak agonist of PPARγ (Berger et al., 2012), it can also produce some weak stimulation of PPARγ. Thus, on the one hand, SB-FI-26 can interfere with fatty acid stimulation of PPARγ; on the other hand, it can also replace fatty acids, which in turn stimulates PPARγ in a much weaker manner. This may explain why SB-FI-26 cannot completely inhibit tumorigenicity and metastasis of CRPC cells (Al-Jameel et al., 2017).

Like SB-FI-26, dmrFABP5 also produces a reduction in the level of p-PPARγ. However, the reduction caused by dmrFABP5 is not through competitively binding to FABP5 (Al-Jameel et al., 2019, Forootan et al., 2016) to block the uptake of the cellular fatty acids. The true mechanism of how dmrFABP5 reduces the biological activity of PPARγ is not fully understood. Previous work showed that

FIGURE 5 The effect of wtrFABP5 and dmrFABP5 on levels of PPARγ, p-PPARγ, AKT, p-AKT, cleaved-Caspase-9 and cleaved-Caspase-3 in PC3 cells. The highly malignant PC3 cells were cultured to 90% confluence and harvested; equal numbers (1×10^5) of cells were then subcultured in triplicate. The optimal dose of wtrFABP5 (0.5 μM) or dmrFABP5 (0.5 μM) was added to each of triplicate cultures and the cells were allowed to grow for 48 h before being harvested and disrupted with cell lysis buffer. Cell extracts were first subjected to SDS-PAGE and then Western blot. An antibody against non-muscle β-actin was incubated with each blot to correct for possible loading discrepancies and for standardization purposes. (A) Western blot of the effects of treatments with PBS (Control), 0.5 μM wtrFABP5 and 0.5 μM dmrFABP5, respectively, on cellular levels of PPARγ (a), p-PPARγ (b), AKT (c), p-AKT (d); Western blot analyses of the effects of treatments with PBS (Control), 0.5 μM wtrFABP5, 0.5 μM dmrFABP5 and combination of 0.5 μM wtrFABP5 and 0.5 μM dmrFABP5, respectively, on cellular levels of cleaved-caspase-9 (e), and cleaved-caspase-3 (f). (B) Quantitative assessments by densitometry scanning of the intensities of the bands representing relative levels of PPARγ (a), p-PPARγ (b), AKT (c), p-AKT (d). The level of the control band (treated with PBS) in each panel was set at 1. The levels in cells treated with 0.5 μM wtrFABP5 and dmrFABP5 were calculated, respectively, by relating to that in control. Quantitative assessments by densitometry scanning of the intensities of the bands representing relative levels of cleaved-Caspase-9 (e) and cleaved-Caspase-3 (f). The results were obtained from 3 (mean ± SD) separate experiments. The level of the control band (treated with PBS) in each panel was set at 1. The levels in cells treated with 0.5 μM wtrFABP5, 0.5 μM dmrFABP5 and combination of 0.5 μM wtrFABP5 and 0.5 μM dmrFABP5 were calculated, respectively, by relating to that in control.

10958355, 0, Downloaded from https://onlinelibrary.wiley.com/doi/10.1002/cbin.11989 by Test, Wiley Online Library on [18/01/2023]. See the Terms and Conditions (https://onlinelibrary.wiley.com/terms-and-conditions) on Wiley Online Library for rules of use; OA articles are governed by the applicable Creative Commons License

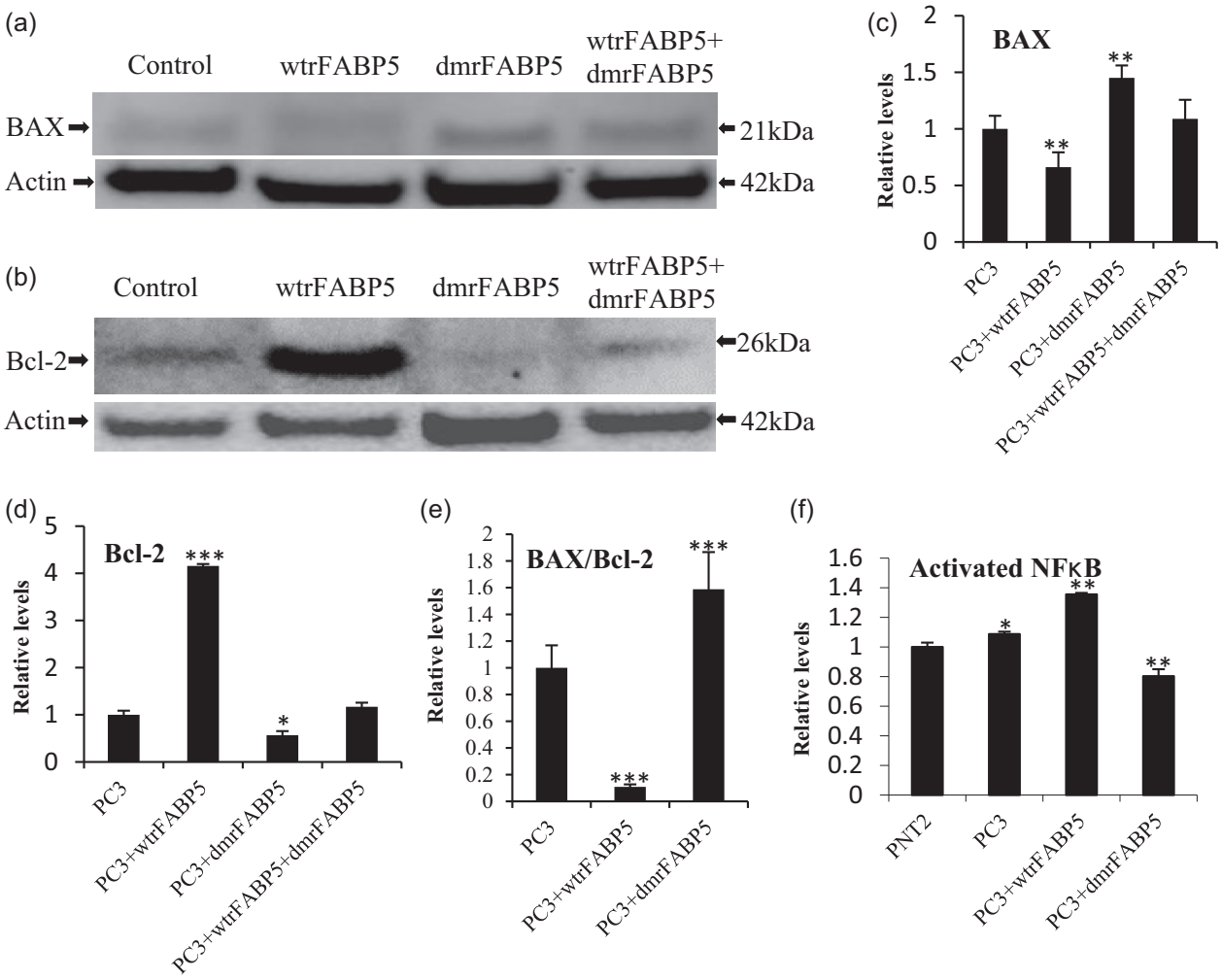

FIGURE 6 The effect of wtrFABP5 and dmrFABP5 on levels of BAX and Bcl-2 and the effect of dmrFABP5 on NF-κB activity in PC3 cells. Western blot analysis of levels of (a) BAX and (b) Bcl-2 in control (treated with PBS), wtrFABP5 (0.5 μM), dmrFABP5 (0.5 μM)-treated cells and combination of 0.5 μM wtrFABP5 and 0.5 μM dmrFABP5 (c, d). Quantitative analysis of the relative levels of BAX and Bcl-2 by densitometric scanning of the intensities of the bands on the blot relative to those of actin. The level of the band for each internal control was set at 1. (e) Ratio of BAX/Bcl-2. The ratio of BAX/Bcl-2 in the untreated control cells was set at 1. (f) The effect of dmrFABP5 on NF-κB activity in PC3 cells. NF-κB transcription factor assay was conducted to test the effect of dmrFABP5 on NF-κB activity. The highly malignant cell line PC3 and benign cell line PNT2 were cultured to 90% confluence and harvested; equal numbers (1×10^5) of cells were then sub-cultured in triplicate. DmrFABP5 (0.5 μM) was added to each of the triplicate PC3 cultures and the cells were allowed to grow for 48 h. Cells were then harvested, and the cellular pellets were subjected to nuclear protein extraction with a nuclear extraction kit (Abcam). The complete transcription factor binding assay buffer (CTFB) was prepared as described by the manufacturer. Ten μl (50 μg) of PNT2, PC3 and dmrFABP5-treated PC3 nuclear extracts were added to the sample wells with 90 μl CTFB on Transcription Factor NF-kB coated strips. Positive control, nonspecific binding and specific competitor dsDNA were added to appropriate wells. The loaded transcription factor NF-kB 96-well strip plate was read by a spectrophotometer (SPECTRA max Plus, Molecular Devices). The results were obtained from 3 (mean ± SD) separate experiments. Quantitative analysis of the relative OD each group was made and the OD level of the PNT2 group was set at 1. SD, standard deviation.

it was necessary for the FABPs to contact PPARs physically for an efficient delivery of fatty acids to the PPARs (Hostetler et al., 2009). Since dmrFABP5 has a very similar structure to that of wild type FABP5, it is possible that dmrFABP5 may bind to PPARγ to occupy the physical space for wild type FABP5, thereby preventing the efficient delivery of fatty acids to PPARγ and thus suppress malignant progression (Al-Jameel et al., 2019).

PPARγ is located on the nuclear membrane, it is highly expressed in adipose tissue and plays an important role to regulate adipose tissue formation and insulin sensitivity (Subbarayan et al., 2004). Studies in recent years have confirmed that PPARγ plays a very important role in promoting malignant progression of prostate cancer (Ahmad et al., 2016; Elix et al., 2018). Our previous study suggested that the FABP5-PPARγ-VEGF signaling pathway played a dominant role for transduction of malignant signals in CRPC cells (Forootan et al., 2016). While wtrFABP5 increased p-PPARγ and dmrFABP5 reduced it, the promoting effect of wtrFABP5 on p-PPARγ in prostate cancer cells was completely reversed by dmrFABP5 when

10958355, 0, Downloaded from https://onlinelibrary.wiley.com/doi/10.1002/cbin.11989 by Test, Wiley Online Library on [18/01/2023]. See the Terms and Conditions (https://onlinelibrary.wiley.com/terms-and-conditions) on Wiley Online Library for rules of use; OA articles are governed by the applicable Creative Commons License

both were addedtogether. Thus it was concluded that dmrFABP5 suppressed the tumorigenicity and metastasis by reversing the promoting effect of wtrFABP5 on p-PPARγ (Al-Jameel et al.,2019). In the current study, although the total PPARγ levels in 22Rv1 and PC3 cells were not higher than in the benign PNT2 cells, the activated p-PPARγ levels were significantly higher when measure relative to a housekeeping actin (Figure 3a,c,e,g). The level of p-PPARγ was significantly reduced when PC3 cells were treated with dmrFABP5, but it was significantly increased when they were treated with wtrFABP5. This result suggested dmrFABP5 played an opposite role to wtrFABP5 and suppressed the activation of PPARγ (Figures 5A[c], 5B[c]). Thus, it is possible that the increased apoptosis is caused by the reduction in the levels of p-PPARγ.

To study the molecular mechanism of how p-PPARγ could affect apoptosis, we investigated the effect of p-PPARγ on the PI3K-AKT-signaling pathway, which controls cell survival and apoptosis. In this pathway, AKT has been reported to be activated through the activated PI3K (Franke et al., 1995; Okano et al., 2000; Vivanco &

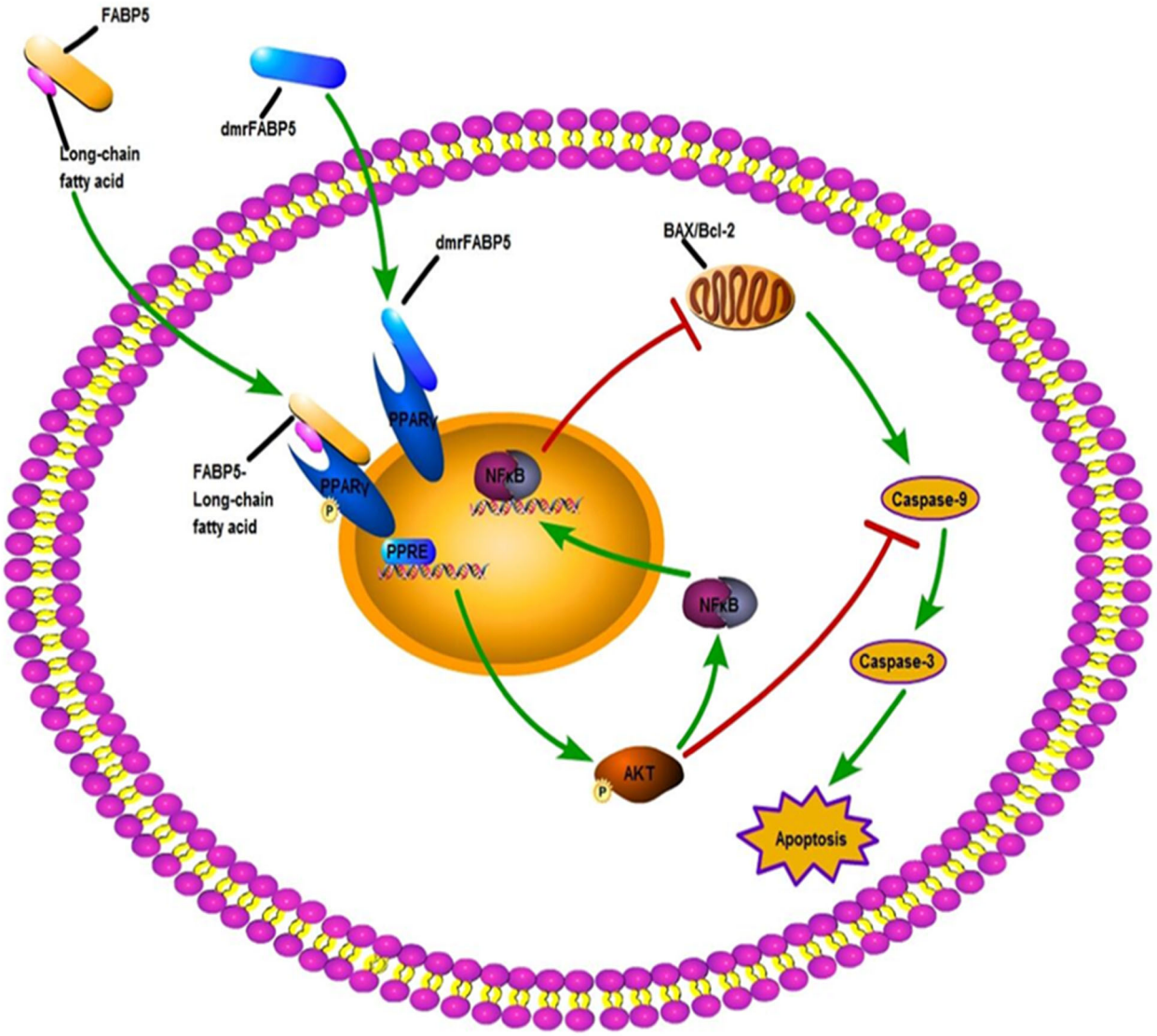

FIGURE 7 Schematic illustration of the possible FABP5-related signaling pathway leading to apoptosis-inhibition and the apoptosis-promoting effect of dmrFABP5 in prostate cancer cells. In untreated prostatic cancer, high level of FABP5 transporting a large amount of fatty acids into cells and binds to PPARγ to deliver the fatty acids and to activate their nuclear receptor PPARγ by phosphorylation. The p-PPARγ may then activate its downstream regulatory target AKT. The p-AKT can suppress apoptosis either by inhibiting the cleavage of caspase-9 or by promoting the activity of NF-κB, which can influence the balance of mitochondrial BAX/Bcl-2 in favors inhibition of apoptosis. DmrFABP5 is incapable of binding to fatty acids, but it has a very similar structure to wtrFABP5. DmrFABP5 may bind to PPARγ in the same way and prevent wtrFABP5 from binding to PPARγ and delivering its fatty acids. This disruption of fatty acid stimulation to PPARγ may lead to a cessation of PPARγ activation. The reduced level of p-PPARγ can lead to an increased p-AKT by losing its suppression. An increased p-AKT may lead to an increase of the apoptosis of cancer cells either by upregulating levels of the cleaved caspase-9 and the cleaved caspase-3 or by suppressing the biological activity of NF-κB, which in turn influences the balance of BAX/Bcl2 in the direction favoring apoptosis-promotion.

10958355, 0, Downloaded from https://onlinelibrary.wiley.com/doi/10.1002/cbin.11989 by Test, Wiley Online Library on [18/01/2023]. See the Terms and Conditions (https://onlinelibrary.wiley.com/terms-and-conditions) on Wiley Online Library for rules of use; OA articles are governed by the applicable Creative Commons License

Sawyers, 2002), which triggers the phosphorylation of AKT at Thr^{308} or Ser^{473} (Alessi et al., 1996). Biologically activated p-AKT activates or inactivates the individual members of the downstream Bcl-family of proteins to disrupt their balance. This leads to a reduced level of caspase-9 and hence suppression of apoptosis (Cardone et al., 1998, Datta et al., 1997; Peso et al., 1997). Although our results show that the total AKT levels are decreased in both the AR^+ CRPC cell line 22Rv1 and AR^- CRPC cell line PC3 compared to that in the benign PNT2 cells relative to actin (Figures 3e,f), the levels of p-AKT are increased (Figures 3g,h). This result suggests that the increased proportion of p-AKT is likely to be obtained by phosphorylation of the reduced proportion of the total or inactivated AKT, rather than gained by producing more total AKT in cells. When PC3 cells are treated with wtrFABP5, the level of p-AKT is significantly increased by 69%, whereas when treated with dmrFABP5, the overall level of p-AKT is significantly reduced by 21% (Figure 5B,b). This result suggests that the reduction in the level of p-PPARγ produced by dmrFABP5 has led to a significant suppression of p-AKT, which eventually may lead to the cleavage of caspase-9 (Figure 5B,d) and promotion of apoptosis. Thus dmrFABP5 promotes apoptosis by reversing the suppressive effect of wtrFABP5.

Some kinases, including AKT, can influence the upstream factors of the NFκB pathway. AKT phosphorylated at Thr^{308} or Ser^{473} upregulates the p65 size subunit of NFκB (Madrid et al., 2001; Suh et al., 2002). Some external stimulations can cause the phosphorylation, ubiquitination and subsequent degradation of IκB proteins, which bind and inhibit the p65 subunit, thereby enabling translocation of NFκB into the nucleus. NFκB transcription factors bind to DNA sequences as dimers to regulate the expression of downstream genes involved in cell growth and apoptosis (Amiri & Richmond, 2005; Pomerantz & Baltimore, 2002; Viatour et al., 2005). In this study (Figure 6f), we have found that the activity of NFκB in the malignant PC3 cancer cells is 9% higher than that in the benign PNT2 cells, suggesting that the apoptosis level is lower and thus the survival pathway is more active in the cancer cells. The wtrFABP5 treatment in PC3 cells increased NFκB activity by 25%, but dmrFABP5 reduced NFκB activity by 27% when compared to the PC3 control (treated with PBS). This result suggests that wtrFABP5 or dmrFABP5 in prostate cancer cells can promote or suppress apoptosis by up- or down-regulation, respectively, of the biological activity of NFκB.

Previous studies have shown that the effect of NFκB activity on apoptosis was achieved by influencing the balance of BAX/Bcl-2 and its subsequent effect on the caspase family, particular caspase-3. Bcl-2 is a crucial suppressor of apoptosis (Hockenbery et al., 1993; Revelos et al., 2005). Bcl-2 and BAX form a heterodimer, which inhibits the function of BAX in promoting apoptosis. Thus, an increased BAX/Bcl-2 ratio indicates an increased percentage of cells undergoing apoptosis. In this study (Figure 6), we observe that the treatment of PC3 cells with wtrFABP5 greatly reduces the level of BAX but increases the level of Bcl-2. In contrast, the treatment with dmrFABP5 significantly increases the level of BAX, but slightly reduces the level of Bcl-2. The wtrFABP5 and dmrFABP5 therefore, when added alone, changed the BAX/Bcl-2 ratio in opposite directions. Whereas wtrFABP5 reduced this ratio to produce a suppressive effect on apoptosis and promote malignant progression; its inhibitors, such as dmrFABP5, increases this ratio to promote apoptosis, which inhibits the malignant progression of the cancer cells.

5 | CONCLUSIONS

By transporting excessive amount of fatty acids to stimulate PPARγ, the increased level of FABP5 upregulates the level of p-PPARγ, which then increases both the level of p-AKT and the biological activity of NFκB in prostate cancer cells. The upregulation of p-AKT and NFκB leads to the reduction of BAX and the subsequent change of the BAX/Bcl-2 ratio; suppresses the cleavages of caspase-9 and caspase-3 and thus inhibits apoptosis and promotes malignant progression. In exact opposite to FABP5, inhibitors SB-FI-26 and dmrFABP5 separately inhibited the level of p-PPARγ by causing the cessation of fatty acid stimulation in one of the two ways: either through competitively binding to fatty acids (SB-FI-26) or a possible obstruction of fatty acid delivery (dmrFABP5). As shown by the schematic illustration in Figure 7, the reduced level of p-PPARγ leads to the suppression of p-AKT and activity of NFκB and an increase in the ratio of BAX/Bcl-2, which in turn increases the levels of cleaved-caspase-9 and cleaved caspase-3 and hence can promote apoptosis and inhibited the malignant progression of the cancer cells.

AUTHOR CONTRIBUTIONS

Jiacheng Zhang, assisted by Gang He, Xi Jin, Bandar T. Alenezi, Abdulghani A. Naeem, and Saud A. Abdulsamad, performed the experimental work. Youqiang Ke designed and supervised the study, prepared the manuscript. Jiacheng Zhang, Gang He, and Xi Jin discussed the results contributed critical suggestions. Jiacheng Zhang also assisted the manuscript writing. All authors read and agreed to this submitted version of the manuscript.

ACKNOWLEDGMENTS

B. T. A. is supported by a PhD studentship from the Faculty of Medicine, Northern Borders University, Saudi Arabia. A. A. N. and S. A. A. are supported by Ph.D scholarships from King Saud Bin Abdulaziz University for Health Sciences, College of Science and Health Professions, Jeddah, Saudi Arabia. The study was not supported by a specific fund. Some consumable costs were met by a joint (G. H. and Y. K.) International Cooperation grant from the Science and Technology Department, Sichuan Province, China (Grant Number: 2019YFH0054).

CONFLICT OF INTEREST

The authors declare no conflict of interest.

DATA AVAILABILITY STATEMENT

The data that support the findings of this study are available from the corresponding author upon reasonable request.

10958355, 0, Downloaded from https://onlinelibrary.wiley.com/doi/10.1002/cbin.11989 by Test, Wiley Online Library on [18/01/2023]. See the Terms and Conditions (https://onlinelibrary.wiley.com/terms-and-conditions) on Wiley Online Library for rules of use; OA articles are governed by the applicable Creative Commons License

ORCID

Youqiang Ke http://orcid.org/0000-0001-5341-8644

REFERENCES

Adamson, J., Morgan, E. A., Beesley, C., Mei, Y., Foster, C. S., Fujii, H., Rudland, P. S., Smith, P. H., & Ke, Y. (2003). High-level expression of cutaneous fatty acid-binding protein in prostatic carcinomas and its effect on tumorigenicity. *Oncogene*, *22*, 2739–2749.

Ahmad, I., Mui, E., Galbraith, L., Patel, R., Tan, E. H., Salji, M., Rust, A. G., Repiscak, P., Hedley, A., Markert, E., Loveridge, C., van der Weyden, L., Edwards, J., Sansom, O. J., Adams, D. J., & Leung, H. Y. (2016). Sleeping beautyscreen revealsppargactivation in metastatic prostate cancer. *Proceedings of the National Academy of Sciences*, *113*, 8290–8295.

Alessi, D. R., Andjelkovic, M., Caudwell, B., Cron, P., Morrice, N., Cohen, P., & Hemmings, B. A. (1996). Mechanism of activation of protein kinase B by insulin and IGF-1. *The EMBO Journal*, *15*, 6541–6551.

Al-Jameel, W., Gou, X., Forootan, S. S., Fayi, M. S. A., Rudland, P. S., Forootan, F. S., Zhang, J., Cornford, P. A., Hussain, S. A., & Ke, Y. (2017). Inhibitor SBFI26 suppresses the malignant progression of castration-resistant PC3-M cells by competitively binding to oncogenic FABP5. *Oncotarget*, *8*, 31041–31056.

Al-Jameel, W., Gou, X., Jin, X., Zhang, J., Wei, Q., Ai, J., Li, H., Al-Bayati, A., Platt-Higgins, A., Pettitt, A., Rudland, P. S., & Ke, Y. (2019). Inactivated FABP5 suppresses malignant progression of prostate cancer cells by inhibiting the activation of nuclear fatty acid receptor PPARγ. *Genes & Cancer*, *10*, 80–96.

Amiri, K. I., & Richmond, A. (2005). Role of nuclear factor-κ B in melanoma. *Cancer and Metastasis Reviews*, *24*, 301–313.

De Angelis, R., Sant, M., Coleman, M. P., Francisci, S., Baili, P., Pierannunzio, D., Trama, A., Visser, O., Brenner, H., Ardanaz, E., Bielska-Lasota, M., Engholm, G., Nennecke, A., Siesling, S., Berrino, F., & Capocaccia, R. (2014). Cancer survival in Europe 1999-2007 by country and age: Results of EUROCARE-5-a population-based study. *The lancet Oncology*, *15*, 23–34.

Bao, Z., Malki, M. I., Forootan, S. S., Adamson, J., Forootan, F. S., Chen, D., Foster, C. S., Rudland, P. S., & Ke, Y. (2013). A novel cutaneous fatty acid-binding protein-related signaling pathway leading to malignant progression in prostate cancer cells. *Genes & Cancer*, *4*, 297–314.

Berger, W. T., Ralph, B. P., Kaczocha, M., Sun, J., Balius, T. E., Rizzo, R. C., Haj-Dahmane, S., Ojima, I., & Deutsch, D. G. (2012). Targeting fatty acid binding protein (FABP) anandamide transporters–a novel strategy for development of anti-inflammatory and anti-nociceptive drugs. *PLoS One*, *7*, e50968.

Berthon, P., Cussenot, O., Hopwood, L., Leduc, A., & Maitland, N. (1995). Functional expression of sv40 in normal human prostatic epithelial and fibroblastic cells—differentiation pattern of nontumorigenic cell-lines. *International Journal of Oncology*, *6*, 333–343.

Biswas, P., Datta, C., Rathi, P., & Bhattacharjee, A. (2022). Fatty acids and their lipid mediators in the induction of cellular apoptosis in cancer cells. *Prostaglandins & Other Lipid Mediators*, *160*, 106637.

Carbonetti, G., Converso, C., Clement, T., Wang, C., Trotman, L. C., Ojima, I., & Kaczocha, M. (2020). Docetaxel/cabazitaxel and fatty acid binding protein 5 inhibitors produce synergistic inhibition of prostate cancer growth. *The Prostate*, *80*, 88–98.

Cardone, M. H., Roy, N., Stennicke, H. R., Salvesen, G. S., Franke, T. F., Stanbridge, E., Frisch, S., & Reed, J. C. (1998). Regulation of cell death protease caspase-9 by phosphorylation. *Science*, *282*, 1318–1321.

Cucchi, D., Camacho-Muñoz, D., Certo, M., Pucino, V., Nicolaou, A., & Mauro, C. (2020). Fatty acids - from energy substrates to key regulators of cell survival, proliferation and effector function. *Cell stress*, *4*, 9–23.

Cussenot, O., Berthon, P., Berger, R., Mowszowicz, I., Faille, A., Hojman, F., Teillac, P., Le Duc, A., & Calvo, F. (1991). Immortalization of human adult normal prostatic epithelial cells by liposomes containing large T-SV40 gene. *Journal of Urology*, *146*, 881–886.

Cussenot, O., Berthon, P., Cochand-Priollet, B., Maitland, N. J., & Le Duc, A. (1994). Immunocytochemical comparison of cultured normal epithelial prostatic cells with prostatic tissue sections. *Experimental Cell Research*, *214*, 83–92.

Datta, S. R., Dudek, H., Tao, X., Masters, S., Fu, H., Gotoh, Y., & Greenberg, M. E. (1997). Akt phosphorylation of BAD couples survival signals to the cell-intrinsic death machinery. *Cell*, *91*, 231–241.

Elix, C., Pal, S., & Jones, J. (2018). The role of peroxisome proliferator-activated receptor gamma in prostate cancer. *Asian Journal of Andrology*, *20*, 238–243.

Ferlay, J., Parkin, D. M., & Steliarova-Foucher, E. (2010). Estimates of cancer incidence and mortality in Europe in 2008. *European Journal of Cancer*, *46*, 765–781.

Forootan, F. S., Forootan, S. S., Gou, X., Yang, J., Liu, B., & Chen, D. (2016). Fatty acid activated PPARγ promotes tumorigenicity of prostate cancer cells by up regulating VEGF via PPAR responsive elements of the promoter. *Oncotarget*, *7*, 9322–9339.

Forootan, F. S., Forootan, S. S., Malki, M. I., Chen, D., Li, G., Lin, K., RUDLAND, P. S., FOSTER, C. S., & KE, Y. (2014). The expression of C-FABP and PPARγ and their prognostic significance in prostate cancer. *International Journal of Oncology*, *44*, 265–275.

Forootan, S. S., Foster, C. S., Aachi, V. R., Adamson, J., Smith, P. H., Lin, K., & Ke, Y. (2006). Prognostic significance of osteopontin expression in human prostate cancer. *International Journal of Cancer*, *118*, 2255–2261.

Franke, T. F., Yang, S.-I., Chan, T. O., Datta, K., Kazlauskas, A., Morrison, D. K., Kaplan, D. R., & Tsichlis, P. N. (1995). The protein kinase encoded by the Akt proto-oncogene is a target of the PDGF-activated phosphatidylinositol 3-kinase. *Cell*, *81*, 727–736.

Fujii, K., Kondo, T., Yokoo, H., Yamada, T., Iwatsuki, K., & Hirohashi, S. (2005). Proteomic study of human hepatocellular carcinoma using two-dimensional difference gel electrophoresis with saturation cysteine dye. *Proteomics*, *5*, 1411–1422.

Furuhashi, M., Tuncman, G., Görgün, C. Z., Makowski, L., Atsumi, G., Vaillancourt, E., Kono, K., Babaev, V. R., Fazio, S., Linton, M. F., Sulsky, R., Robl, J. A., Parker, R. A., & Hotamisligil, G. S. (2007). Treatment of diabetes and atherosclerosis by inhibiting fatty-acid-binding protein aP2. *Nature*, *447*, 959–965.

Gujrati, H., Ha, S., Mohamed, A., & Wang, B. D. (2022). MicroRNA-mRNA regulatory network mediates activation of mTOR and VEGF signaling in African American prostate cancer. *International Journal of Molecular Sciences*, *23*, 2926.

Hockenbery, D. M., Oltvai, Z. N., Yin, X.-M., Milliman, C. L., & Korsmeyer, S. J. (1993). Bcl-2 functions in an antioxidant pathway to prevent apoptosis. *Cell*, *75*, 241–251.

Hostetler, H. A., McIntosh, A. L., Atshaves, B. P., Storey, S. M., Payne, H. R., Kier, A. B., & Schroeder, F. (2009). L-FABP directly interacts with PPARα in cultured primary hepatocytes. *Journal of Lipid Research*, *50*, 1663–1675.

Jing, C., Beesley, C., Foster, C. S., Chen, H., Rudland, P. S., West, D. C., Fujii, H., Smith, P. H., & Ke, Y. (2001). Human cutaneous fatty acid-binding protein induces metastasis by up-regulating the expression of vascular endothelial growth factor gene in rat Rama 37 model cells. *Cancer Research*, *61*, 4357–4364.

Jing, C., Beesley, C., Foster, C. S., Rudland, P. S., Fujii, H., Ono, T., Chen, H., Smith, P. H., & Ke, Y. (2000). Identification of the messenger RNA for human cutaneous fatty acid-binding protein as a metastasis inducer. *Cancer Research*, *60*, 2390–2398.

Kaighn, M. E., Lechner, J. F., Narayan, K. S., & Jones, L. W. (1978). Prostate carcinoma: Tissue culture cell lines. *National Cancer Institute Monograph*, 17–21.

10958355, 0, Downloaded from https://onlinelibrary.wiley.com/doi/10.1002/cbin.11989 by Test, Wiley Online Library on [18/01/2023]. See the Terms and Conditions (https://onlinelibrary.wiley.com/terms-and-conditions) on Wiley Online Library for rules of use; OA articles are governed by the applicable Creative Commons License

Ke, Y., Jing, C., Barraclough, R., Smith, P., Davies, M. P. A., & Foster, C. S. (1997). Elevated expression of calcium-binding protein p9Ka is associated with increasing malignant characteristics of rat prostate carcinoma cells. *International Journal of Cancer*, *71*, 832–837.

Lee, J. T., Lehmann, B. D., Terrian, D. M., Chappell, W. H., Stivala, F., Libra, M., Martelli, A. M., Steelman, L. S., & McCubrey, J. A. (2008). Targeting prostate cancer based on signal transduction and cell cycle pathways. *Cell Cycle*, *7*, 1745–1762.

Levi, L., Wang, Z., Doud, M. K., Hazen, S. L., & Noy, N. (2015). Saturated fatty acids regulate retinoic acid signalling and suppress tumorigenesis by targeting fatty acid-binding protein 5. *Nature Communications*, *6*, 8794.

Li, J., Simpson, L., Takahashi, M., Miliaresis, C., Myers, M. P., Tonks, N., & Parsons, R. (1998). The PTEN/MMAC1 tumor suppressor induces cell death that is rescued by the AKT/protein kinase B oncogene. *Cancer Research*, *58*, 5667–5672.

Liu, R. Z., Choi, W. S., Jain, S., Dinakaran, D., Xu, X., Han, W. H., Yang, X. H., Glubrecht, D. D., Moore, R. B., Lemieux, H., & Godbout, R. (2020). The FABP12/PPARγ pathway promotes metastatic transformation by inducing epithelial-to-mesenchymal transition and lipid-derived energy production in prostate cancer cells. *Molecular oncology*, *14*, 3100–3120.

Liu, R. Z., & Godbout, R. (2020). An amplified fatty Acid-Binding protein gene cluster in prostate cancer: Emerging roles in lipid metabolism and metastasis. *Cancers*, *12*, 3823.

Madrid, L. V., Mayo, M. W., Reuther, J. Y., & Baldwin, A. S. (2001). Akt stimulates the transactivation potential of the RelA/p65 subunit of NF-κB through utilization of the IκB kinase and activation of the mitogen activated protein kinase p38. *Journal of Biological Chemistry*, *276*, 18934–18940.

Madsen, P., Rasmussen, H. H., Leffers, H., Honoré, B., & Celis, J. E. (1992). Molecular cloning and expression of a novel keratinocyte protein (psoriasis-associated fatty acid-binding protein [PA-FABP]) that is highly up-regulated in psoriatic skin and that shares similarity to fatty acid-binding proteins. *Journal of Investigative Dermatology*, *99*, 299–305.

McKillop, I. H., Girardi, C. A., & Thompson, K. J. (2019). Role of fatty acid binding proteins (FABPs) in cancer development and progression. *Cellular Signalling*, *62*, 109336.

Miyamoto, H., Messing, E. M., & Chang, C. (2004). Androgen deprivation therapy for prostate cancer: Current status and future prospects. *The Prostate*, *61*, 332–353.

Morgan, E. A., Forootan, S. S., Adamson, J., Foster, C. S., Fujii, H., Igarashi, M., Beesley, C., Smith, P. H., & Ke, Y. (2008). Expression of cutaneous fatty acid-binding protein (C-FABP) in prostate cancer: Potential prognostic marker and target for tumourigenicity-suppression. *International Journal of Oncology*, *32*, 767–775.

Naeem, A. A., Abdulsamad, S. A., Rudland, P. S., Malki, M. I., & Ke, Y. (2019). Fatty acid-binding protein 5 (FABP5)-related signal transduction pathway in castration-resistant prostate cancer cells: A potential therapeutic target. *Precision Clinical Medicine*, *2*, 192–196.

Okano, J., Gaslightwala, I., Birnbaum, M. J., Rustgi, A. K., & Nakagawa, H. (2000). Akt/protein kinase B isoforms are differentially regulated by epidermal growth factor stimulation. *Journal of Biological Chemistry*, *275*, 30934–30942.

Peso, L., González-García, M., Page, C., Herrera, R., & Nuñez, G. (1997). Interleukin-3-induced phosphorylation of BAD through the protein kinase Akt. *Science*, *278*, 687–689.

Pomerantz, J. L., & Baltimore, D. (2002). Two pathways to NF-κB. *Molecular Cell*, *10*, 693–695.

Revelos, K., Petraki, C., Gregorakis, A., Scorilas, A., Papanastasiou, P., & Koutsilieris, M. (2005). Immunohistochemical expression of Bcl2 is an independent predictor of time-to-biochemical failure in patients with clinically localized prostate cancer following radical prostatectomy. *Anticancer Research*, *25*, 3123–3133.

Sinha, P., Hütter, G., Köttgen, E., Dietel, M., Schadendorf, D., & Lage, H. (1999). Search for novel proteins involved in the development of chemoresistance in colorectal cancer and fibrosarcoma cells in vitro using two-dimensional electrophoresis, mass spectrometry and microsequencing. *Electrophoresis*, *20*, 2961–2969.

Sramkoski, R. M., Pretlow, T. G., 2nd, Giaconia, J. M., Pretlow, T. P., Schwartz, S., Sy, M. S., Marengo, S. R., Rhim, J. S., Zhang, D., & Jacobberger, J. W. (1999). A new human prostate carcinoma cell line, 22Rv1. *In Vitro Cellular & Developmental Biology. Animal*, *35*, 403–409.

Subbarayan, V., Sabichi, A. L., Kim, J., Llansa, N., Logothetis, C. J., Lippman, S. M., & Menter, D. G. (2004). Differential peroxisome proliferator-activated receptor-gamma isoform expression and agonist effects in normal and malignant prostate cells. *Cancer Epidemiology, Biomarkers & Prevention: A Publication of the American Association for Cancer Research, cosponsored by the American Society of Preventive Oncology*, *13*, 1710–1716.

Suh, J., Payvandi, F., Edelstein, L. C., Amenta, P. S., Zong, W. X., Gélinas, C., & Rabson, A. B. (2002). Mechanisms of constitutive NF-κB activation in human prostate cancer cells. *The Prostate*, *52*, 183–200.

Viatour, P., Merville, M.-P., Bours, V., & Chariot, A. (2005). Phosphorylation of NF-κB and IκB proteins: Implications in cancer and inflammation. *Trends in Biochemical Sciences*, *30*, 43–52.

Vivanco, I., & Sawyers, C. L. (2002). The phosphatidylinositol 3-kinase–AKT pathway in human cancer. *Nature Reviews Cancer*, *2*, 489–501.

Vorum, H., Madsen, P., Svendsen, I., Celis, J. E., & Honoré, B. (1998). Expression of recombinant psoriasis-associated fatty acid binding protein in *Escherichia coli*: Gel electrophoretic characterization, analysis of binding properties and comparison with human serum albumin. *Electrophoresis*, *19*, 1793–1802.

How to cite this article: Zhang, J., He, G., Jin, X., Alenezi, B. T., Naeem, A. A., Abdulsamad, S. A., & Ke, Y. (2023). Molecular mechanisms on how FABP5 inhibitors promote apoptosis-induction sensitivity of prostate cancer cells. *Cell Biology International*, 1–14. https://doi.org/10.1002/cbin.11989

10958355, 0, Downloaded from https://onlinelibrary.wiley.com/doi/10.1002/cbin.11989 by Test, Wiley Online Library on [18/01/2023]. See the Terms and Conditions (https://onlinelibrary.wiley.com/terms-and-conditions) on Wiley Online Library for rules of use; OA articles are governed by the applicable Creative Commons License